Fermi National Accelerator Laboratory

FERMILAB-FN-590

Exploring Bifurcations in the Four-Dimensional, Off-Centered Beam-Beam Interaction

Leo Michelotti and Selcuk Saritepe

Fermi National Accelerator Laboratory
P.O. Box 500, Batavia, Illinois 60510

June 1992

Submitted to *Physical Review*

Operated by Universities Research Association Inc. under Contract No. DE-AC02-76CHO3000 with the United States Department of Energy

Disclaimer

EXPLORING BIFURCATIONS IN THE FOUR-DIMENSIONAL, OFF-CENTERED BEAM-BEAM INTERACTION

Leo Michelotti and Selcuk Saritepe

Fermi National Accelerator Laboratory

Batavia, Illinois 60510

During Fermilab's current collider run a beam separation scheme will be implemented in the Tevatron employing non-planar, helical orbits. In the course of studying off-centered beam-beam interactions we observed (a) detailed bifurcations of separatrices in four-dimensional transverse phase space, (b) phaselocked, "irregular" resonant orbits, and (c) exceedingly weakly chaotic orbits. We report these observations and discuss briefly other collider issues related to off-centered beam-beam interactions: (a) tune shift and (b) perturbations and splitting of the closed orbit.

PACS numbers: 29.20.Lq, 29.27.Bd, 29.50.+v, 29.85.+c, 46.10.+z

I. INTRODUCTION

In the 1988-89 collider run at Fermilab, six antiproton bunches collided head-on with six proton bunches at twelve sites placed symmetrically around the Tevatron. Only the one at the CDF detector (B0) was productive for physics, the other eleven having the negative effect of contributing to a total beam-beam induced tune shift and spread of 0.024, large enough to cover much of the working area between the 5^{th} and 7^{th} order resonances lines. In order to reduce the tune spread and allow us to increase current and luminosity in the Tevatron during the 1992 collider run, proton and antiproton bunches, while still occupying the same beampipe, will be separated everywhere except at two interaction regions (IRs), B0 and D0. Separation schemes have been employed before, at CESR and at the SPS, but Fermilab's will have the unique feature of being fully two-dimensional: the fiducial (design) closed orbits will have the topology of a double helix that is pinched at the IRs, with protons moving on one branch, antiprotons on the other. At sites where opposing bunches will encounter each other they will be separated by approximately five transverse bunch widths, on the average. The number of bunches per beam will remain six in the 1992 collider run but plans exist to increase this eventually to thirty-six. With $33 - 50 \times 10^{10}$ protons and 6×10^{10} antiprotons per bunch, and assuming $\beta^* \approx 50$ cm, this would increase the luminosity to 5×10^{31} cm^{-2}sec^{-1}.

Theoretical and experimental studies were conducted to study orbit stability, in the weak-strong approximation, under the double-helix scenario.[14, 17] A "probe" antiproton experiences nonlinear kicks from a sequence of "source" proton bunches, and vice versa. Parity of the beam-beam interaction is broken because the fiducial (design closed) orbits of the two species do not coincide, so all resonances can be excited. The effects are distributed, much like those of small nonlinear fields distributed around the ring, and we can expect resonances to play a role in the resultant motion.

The principal observations reported here are (a) bifurcations of chaotic separatrices leading to (b) the existence of very low entropy chaotic orbits. The "control parameter" for these bifurcations was the separator strength, which controlled the size of the double helix. However, before we proceed to discuss these, we shall briefly summarize a few practical matters concerning closed orbit distortions and tune spread.

II. COLLIDER CONSIDERATIONS

The practical, engineering results of our studies, some of which have been reported elsewhere [14] were presented at a DoE review in August, 1989 [10]. While not summarizing these in detail, we shall quickly touch upon a few important features in connection with closed orbit distortion, tune shift, and closed orbit bifurcations.

• **closed orbit** One of the most critical issues was the distortion of proton and antiproton closed orbits produced by the multiple, off-centered beam-beam interactions. Deviations from the fiducial orbits will obviously be negligibly small at all encounter sites except the two crucial ones: the IRs, where the fiducial orbits coincide for a space of ≈ 50 meters. Significant fluctuations away from this coincidence would lead to decreased luminosity and possible instability. Exact closed orbits, including the off-centered beam-beam interactions, were calculated at B0 and D0 using Newton's method to converge on the solution; Jacobians were obtained using automated differentiation.[12] For reasonable scenarios — say, 36×36 with 6×10^{10} protons per bunch — the displacement at full excitation was 10%, or less, of the transverse bunch width.[14] Angular offsets of the closed orbit were similarly small: letting ψ represent the tilt angle of the closed orbit, relative to the fiducial orbit, we typically found that

$$\begin{aligned} \psi &\approx 0.5 \frac{\sigma}{\beta^*} \\ &= 0.5 \frac{\sigma}{l} \frac{l}{\beta^*} \end{aligned}$$

where l is the bunch length, σ is the transverse bunch width (rms), and β^* is the envelope lattice function at the IR. If we take $l/\beta^* \approx O(1)$ and $4\sigma/l = (2\sigma)/(l/2) \equiv \theta_{\rm bunch}$ as a "maximum" possible angle subtended by a particle passing through the 1σ region of the bunch we get

$$\psi \approx 0.1\,\theta_{\rm bunch} \ .$$

Interpreted in this way, the angle subtended by the closed orbit of the (probe) bunch is only about 10% of the total available proton bunch angle.

Following a similar line of reasoning for individual particles in the bunch, leads to a more interesting conclusion. If the probe particles are assumed to lie on an invariant phase space distribution *before* taking the beam-beam kicks into account, then it must be that at D0

$$\begin{aligned}\sigma_{y'} &= \sigma_y/\beta^* \\ &= (\sigma_y/l)(l/\beta^*) \\ &\approx \frac{1}{4}\theta_{\rm bunch} \ .\end{aligned}$$

β^* is so small that particles within the probe bunch are traversing the source bunch at angles that are 25%, or so, of $\theta_{\rm bunch}$, in contradiction to the basic assumption of parallel passage through the source bunch, which is required for the derivation of Montague's beam-beam kick.[15] The kick approximation is not valid for low beta collisions. A second objection to Montague's kick follows from the observation that β, and therefore σ, is changing rapidly in the low-beta region. Because of this, antiprotons at the head or tail of the bunch will experience different beam-beam forces than those in the center. However, in both cases, the error we make is in the right direction: we are ignoring both the dependence on x' and y' and the larger transverse bunch widths — and weaker beam-beam kicks — on either side of of the IRs. Using

impulsive kicks tends to overestimate the effects of beam-beam interactions; in this sense it is a "conservative" approximation. Momentum transfers more appropriate to oblique passage through a bunch have been studied by Krishnagopal and Siemann [6] and by Kheifets and Voss [5].

• **tune shift and spread** Because the closed orbit was found via an application of Newton's method, we simultaneously had available, in the Jacobians, all the information necessary to compute small-amplitude tune shifts induced by the beam-beam interactions. These numbers also indicate the tune *spread* in a bunch, since the particles closest to the center undergo the full tune shift while that of those at large amplitudes is negligible. These results were extended and checked later by direct simulation and machine studies.[17]

When separators are off and the helix is closed, proton tunes shifted by ≈ 0.13, which was the amount expected from the simple formula for round beams,

$$\xi = 0.007\, N[10^{10}]/\epsilon_{\rm inv}[\pi\ {\rm mm} - {\rm mr}]$$

for the beam-beam tune shift per collision at 900 GeV. (On the other hand, the maximum tune shift for antiprotons was *smaller* than expected, an effect which we shall return to below.) As separators achieve their full voltage, these tunes drop quickly to those expected from the two head-on collisions plus a little extra from the long-range beam-beam interactions.

Using the small-amplitude tune shifts as a calibration check, and with the helix fully open, comparisons were made between beam-beam tune shifts obtained by (a) Fourier analyzing the orbits arising from simulation (tracking) and (b) semi-analytic calculation using an integral expression based on neglecting all contribution except the two direct beam-beam interactions at the IRs. Derivation of this integral expression, originally due to Bambade [1], is given in the Appendix. The amplitude

dependence of the tune shift was in excellent agreement, but the simulated tune shift was systematically about 0.004 above the calculated one. That this indeed arose from the off-centered collisions was checked by direct computation in the following way. The long range part of the beam-beam impulse, obtained by omitting the exponential piece, has a $1/r$ dependence.

$$\Delta \underline{r}'[10^{-8}] = -2.9 \left(N[10^{10}]/E[\mathrm{TeV}] \right) \left(\underline{r}/|\underline{r}|^2 \right) [\mathrm{mm}^{-1}] \ ,$$

Here N is the number of protons per source bunch, E is the energy per proton, and $\underline{r}$ is the two-dimensional transverse vector from the center of the source bunch to the probe particle. This can be thought of as arising from a magnetic field whose effective multipole content is obtained by expanding $\underline{r} = \underline{d} + \underline{u}$, where $\underline{d}$ is the offset between beams, and thinking of this as a relation between complex variables rather than two-dimensional vectors. The effective multipole components of this kick are then written in the following convenient fashion.

$$\frac{B_o R}{B\rho} \int d\theta \ (b_n + i a_n) = 2.9 \times 10^{-11} \mathrm{m} \ \frac{N[10^{10}]}{E[\mathrm{TeV}]} \ (-1)^n \ (1/d)^{n+1}$$

Note well that d in this formula is the complex number $x + iy$, where x and y are the components of $\underline{r}$. Plugging in the numbers appropriate to our model, $N = 33$, $E = 1$, and setting $n = 1$ (quadrupole), the normal quadrupole effective strength became,

$$\left. \frac{B'l}{B\rho} \right|_{\mathrm{effective}} [\mathrm{m}^{-1}] = -9.6 \times 10^{-4} \ \frac{x^2 - y^2}{(x^2 + y^2)^2} \ [\mathrm{mm}^{-2}] \ .$$

The expected tune shift from this effective quadrupole "error" is given by the following expression.

$$|\delta\nu|_{\text{long range}} = \frac{1}{4\pi} \left| \sum \beta_x \frac{B'l}{B\rho} \right|$$

where the sum is taken over the seventy long range beam-beam hits. The value obtained, 0.0044, completely accounted for the discrepancy between theory and simulation. Even with increased number of bunches, the tune shift induced by the extra

beam-beam "encounters" was only about half of that attributable to one head-on collision.

The tune spread was not appreciably influenced by the long-range collisions. This was as expected, as their contributions should be down by two powers of σ/d compared to the tune shift.

• **closed orbit bifurcation** The zero-amplitude tunes of both protons and antiprotons behaved in a similar manner, but the "closed helix" tune shifts of the antiprotons were much lower than expected. Resolution of this discrepancy involved the bifurcation of the antiproton closed orbit. By following the evolution of proton and antiproton closed orbits as the helix was adiabatically closed we observed that the proton closed orbit returned to its fiducial, passing through the center of the IR, but that of the antiprotons *did not.* Rather, it approached one of a limiting family of closed orbits which were displaced from the fiducial orbit by approximately one transverse bunch width. Further study led to the conclusion that the antiproton fiducial orbit had become unstable as the tune shift became so large that the tune passed an integral value. Although this was not anticipated, it should have been. The phenomenon is not much different from the usual stop-band phenomenon of linear instability, in which the fiducial orbit also becomes unstable. The difference here is that the nonlinearity of the interaction enables closed orbits to move out from the center. These elliptic, off-centered closed orbits explained the "discrepancy" between the calculated and expected tune shifts. The tunes we were observing were associated with them, not with the fiducial orbit, which was no longer stable.

III. TRACKING A SEPARATRIX

The graphical exploration of phase space has been a standard practice in accelerator physics since the 1950's. With the rapid development of modern computer

graphics during the past fifteen years, or so, this visual display of information has gained increased acceptance even among pure mathematicians as a way of gaining insight into the behavior of dynamical systems. After preliminary exploration in which the analyst observes the existence of phase space structures — fixed points, periodic orbits, attractors, resonant orbits, separatrices — analytic models are employed in order to "explain" these structures. The importance of these graphics-based exploratory activities lies in providing the analyst with limited, focussed objectives: identified structures or phenomena which characterize behavior, *and whose existence would have been difficult (or almost impossible) to discover using analysis alone.*

Exploring phase space is greatly facilitated if the graphics are designed for more than display, that is, if one can employ graphical input as well as output. This is especially true when going beyond simple, and generally inadequate, two-dimensional models. In particular, finding the separatrices of four-dimensional Hamiltonian systems and following them through bifurcations are not trivial tasks. They were accomplished graphically here using AESOP, a Phigs-based graphics shell written for the exploration of four-dimensional phase space mappings.[13, 14, 18] A typical AESOP screen is displayed in Figure 1. It shows orbits, each marked with a different color for identification, in the vicinity of a separatrix of the $2\nu_1 - 2\nu_2$ resonance generated by the centered beam-beam interaction. The top two viewports contain two-dimensional projections of four-dimensional transverse phase space: the upper left (right) shows orbits projected along normalized horizontal, x-x' (vertical, y-y') coordinates. The coordinates for the three-dimensional, perspective projections in the lower viewports are the horizontal and vertical "angle" coordinates and an "action" coordinate – which is more an amplitude squared than a true action – horizontal action in the left hand plot and vertical in the right. These coordinates are obtained by expressing the two-dimensional projections in polar, rather than Cartesian, coordinates, the ac-

tions being equivalent to radius squared. These "angle-angle-action"plots have been used before, for example in references [7, p.278], [14] and [16], and are particularly good for exploring resonance structure. Initial conditions for orbits are chosen graphically, either by using traditional two-dimensional cursors in the top two viewports or a specially programmed four-dimensional cursor which is bound to the bottom two (three-dimensional) projections. The low entropy orbits referred to in the introduction were observed by accident several years ago [14] but it was the introduction of the four-dimensional cursor which made it possible to follow the bifurcations that lead up to them.

Some care must be taken in interpretation. For example, the "tube"-like structures are actually two-dimensional tori; in particular, the two red tubes just left and right of center actually belong to the *same* torus. We are viewing a projection of angle data which gets wrapped with 2π periodicity. The blue and gold orbits are exceedingly close to a separatrix: the blue is within a thin chaotic layer associated with the separatrix and visits both its upper and lower branches in the figure; the gold is a regular torus which lies just "outside" this layer. Unlike the the red and yellow tori, their angle coordinates span full range. The four "lobes" which they mark actually represent only two stable regions, one containing the red torus, the other, the yellow; the pieces at the extreme ends are attached to the latter. The evident anti-correlation in horizontal and vertical action coordinates is exactly what is expected from a first order resonance model of a difference resonance. Two stable resonant orbits exist within the yellow and red tori near the regions $S_1 : \varphi_1 - \varphi_2 \simeq 0$ (yellow) and $S_2 : \varphi_1 - \varphi_2 \simeq \pi$ (red); two unstable resonant orbits lie between these near the intersections of the blue and gold orbits, near $U_1 : \varphi_1 - \varphi_2 \simeq \pi/2$ and $U_2 : \varphi_1 - \varphi_2 \simeq 3\pi/2$.

A. Bifurcations and resonant seeding

We turn now to the bifurcations of the separatrix as the helix is opened and all but two of the beam-beam interactions become off-centered. This is an academic thought experiment — a partially opened helix with both proton and antiproton bunches present is not a scenario for collider operations — and this section should be considered akin to a report of its more interesting results. In keeping with the exploratory mode, we shall merely record our observations here, not perform detailed analysis.

The configuration of Figure 1 corresponds to zero separation: all beam-beam collisions are centered (head-on). Figure 2 shows an orthographic projection of the lower left hand viewport seen along the $\varphi_1 = \varphi_2$ diagonal. (φ_1 is the horizontal and φ_2 the vertical angle coordinates.) The thickness of the "tubes" in regions S_1 and S_2 is an artifact produced by the slight ripple seen most prominently in the yellow torus of Figure 1 and could be removed by using a better set of coordinates, obtainable via normal form algorithms.[2, 3] The separatrix, on the other hand, is legitimately chaotic, albeit weakly. Nonetheless, the shape is what one expects from the resonant normal form of a first order perturbation theory, which supports the notion of "resonant seeding" in four dimensions, a point to which we shall return later.

Although the orbits in regions S_1 and S_2 appear similar in this projection they can be very different, depending on the tunes. The slightly rotated, perspective view of Figure 3(a) shows tori surrounding S_1 which are banded — indicating a hierarchy of resonances — winding around the "principal" tori, while the stable, resonant orbit in region S_2 is actually a family of period eight orbits strung together. The small tori appearing in Figure 3(b) surround one member of this family. Now, periodic orbits could be found semi-analytically via Newton's method applied to the appropriate

iterate of the map. Primary resonant orbits, like the one heading down the center of Figure 2, cannot be found directly via Newton's method, as they are not necessarily periodic. However, they could be located approximately by a resonance analysis. The banded tori of S_1 are more complicated. Three levels of resonant behavior are identifiable from the figure. The primary one is the $2\nu_1 - 2\nu_2$ resonance which is partially straightened by the action-angle coordinates used for the projection. The screw-like tori appearing in Figure 3(a) indicate a secondary level of resonance, and a tertiary level is observed in the "inner" one, which is itself striated. Discussions of resonances and resonance behavior usually limit themselves to the primary level, which is typically associated with a line on a tune diagram, of the form $\underline{m} \cdot \underline{\nu} + n = 0$. The local action-angle coordinates which would straighten the secondary or tertiary resonances, cannot be mapped one-to-one onto those of the primary resonance. The authors know of no practical analytic way to *discover* the existence of non-primary resonances, such as those appearing in the banded tori of Figure 3(a), other than to find and display them via graphics-based exploration.

As the helix begins to open and the beam-beam interactions become off-centered, the first global bifurcation takes place, as illustrated in Figure 4. The separatrix no longer connects the two unstable resonant orbits but has split into two branches, each of which is attached to one of them: the central "inverted figure eight" and its "cocoon." The situation may be even more complicated: there is a suggestion that the unstable resonant orbit U_1 has itself split into two.

As the separation increases, a second bifurcation occurs in the vicinity of the unstable resonant orbit U_2. (See Figure 5) Rather then forming the "cocoon" of Figure 4 the branch closes quickly, forming a new figure eight. Unlike the previous bifurcation, this is not one which takes a heteroclinic branch and changes it into a homoclinic one. The branch is homoclinic both before and after the bifurcation; what

has changed is how it closes back on itself at large amplitudes, analagous to what happens when one changes the sign of a shear term in a two-dimensional problem.

This structure may be connected with the creation of "irregular" resonant orbits, which typically are confined to a plane, either near-horizontal or near-vertical.[1] They can arise from a resonant normal form Hamiltonian, say of the form

$$H = H_0(\underline{I}) + H_1(\underline{I})\cos(\underline{m}\cdot\underline{\varphi})$$

by setting H_1, the coefficient of the phase-dependent term, to zero. Unlike regular resonant orbits, which might arise by setting $\underline{m}\cdot\underline{\varphi} = \pi$, for example, their resonant combination of phase coordinates may depend on the system's parameters, and one of their amplitude coordinates, I_1 or I_2, frequently vanishes, which is what confines the motion to a plane. The branch of the separatrix connecting these "irregular" resonances tends to be more phaselocked than normal. Shown in Figure 6 is a rather clean example of an orbit close to such a separatrix, observed in this system but with the helix opened wide enough to make the dynamic less chaotic. The orbit spends most of its time with the relative phase locked at $\varphi_1 - \varphi_2 \simeq 0$ or $\varphi_1 - \varphi_2 \simeq \pi$, the transitions between these two regions taking place comparatively rapidly. Spatially, this corresponds to a a near-planar orbit whose plane slowly oscillates between the horizontal and vertical directions: as the amplitude in one plane goes through zero, the corresponding phase jumps rapidly through π. The alternative extreme would be an orbit whose relative phase was locked at $\varphi_1 - \varphi_2 \simeq \pm\pi/2$, which would pass through a circular intermediate state.

Even though this system is non-integrable and its separatrices are chaotic, they exhibit patterns of bifurcation which are essentially identical with those found in

[1]This terminology is not standard; it was introduced in reference [11]. Stated more precisely, the orbit's samples, which are its Poincaré sections, lie in a plane.

integrably resonant systems.[9] That they do so is observational support for the idea of "resonant seeding": the notion that chaotic layers in the stability boundary of non-integrable systems are built up around and dominated by separatrices that can be associated with underlying, integrable or near-integrable, usually low-order resonance normal forms.[11, 8] In particular, when the system is unstable at large amplitudes, the "boundary layer" between stability and instability — what is usually called the "dynamic aperture" — is frequently associated with the separatrices from these low order resonances. This is an idea which has had some numerical confirmation in two dimensional phase space [8, 4]; we now see evidence for it in four dimensions as well.

B. Unravelled tori: small entropy chaos

The most interesting effect which we observed was that tori in region S_2 appeared to "unravel" as the helix opened. Representative orbits of this kind are shown in Figure 7. They look much like long, tangled threads and are almost periodic, with period five: watching one develop on the screen would reveal that it almost returns on itself after five iterations. This periodicity is clear from the static figure as well, and it would show up as a huge spike in any spectral analysis. Correspondingly, the lengthening of the "thread" is slow; hundreds of iterations may be required to form a single "loop." From the standpoint of the theory of chaos, we may interpret this orbit as chaotic with exceedingly small KS entropy, or a near-zero Lyapunov exponent. That is, these "tangled" orbits are "almost but not quite" regular; they seem, at least superficially, much like one-dimensional objects and do not have the "random" appearance one normally associates with chaotic orbits.

No "tangled" orbits appeared in region S_1. While we do not understand the physical mechanism that produces such orbits or makes the distinction between S_1 and S_2, we conjecture that S_2 contained orbits which sample the core of the source bunches

more frequently. To test this, we recorded χ^2, the bunch separation normalized to the local bunch size, at individual beam-beam encounters for orbits in both regions. Figure 8 shows two typical results, and there is some indication that the guess is correct. If so, the conceptual picture which emerges is this: the ordinary tori of S_1 spend most of their existence at encounter ranges near $\chi \approx 3^+$ while a tangled orbit spends significant time either much closer, $\chi \approx 2$, or much further out, $\chi > 5$. When encounters are at great distances, the tangled orbit lies on one of a family of KAM tori whose tunes happen to be near a fifth integer. When the particle experiences a close encounter, it can jump from one torus in this family to another. We conjecture that this mechanism, in conjunction with the fact that the orbit is almost periodic (with period 5), gives the orbit its extraordinary appearance.

IV. CLOSING REMARKS

Exploring the phase space of the distributed, off-centered beam-beam interaction has revealed both phenomena which are variations on old themes and one that is perhaps new: the "tangled" orbits, exhibiting very low entropy chaos. Chaotic separatrices in four-dimensions have been observed to bifurcate in ways which mimic low order integrable resonances. The next step would be to return to analysis and confirm four-dimensional resonant seeding analytically by computing the separatrices of low order resonant normal form Hamiltonians and comparing them to the observed ones.

ACKNOWLEDGMENTS

This work was performed at Fermi National Accelerator Laboratory which is operated by Universities Research Association Inc. under contract with the United States Department of Energy.

APPENDIX: CENTERED BEAM-BEAM TUNESHIFTS

In the case of a centered (head-on) beam-beam interaction, an integral representation can be written for the tune shift. Begin with the following Hamiltonian.

$$H(\underline{\phi}, \underline{I}; \theta) = \underline{\nu} \cdot \underline{I} + \sum_{\theta_{bb}} U(\underline{x})\, \delta_{2\pi}(\theta - \theta_{bb})$$

This models a decoupled storage ring with horizontal and vertical tunes $\underline{\nu} = (\nu_1, \nu_2)$; each θ_{bb} marks the location of a beam-beam encounter, treated as impulses, with $\delta_{2\pi}$ being a 2π-periodic delta function. The ordered pair $\underline{x} = (x_1, x_2)$ are transverse coordinates and can be obtained from the "action-angle" coordinates $\underline{\phi}$ and $\underline{I}$ according to the prescription,

$$x_k = \sqrt{2 I_k \beta_k(\theta)}\, \sin(\psi_k(\theta) - \nu_k \theta + \phi_k), \quad k = 1, 2, \tag{A1}$$

where β and ψ are Courant-Snyder lattice functions. We use the Montague form for the potential U arising from *offset*, normally oriented, Gaussian bunch.[15]

$$U(\underline{x}) = \lambda \int_0^\infty dt \prod_{k=1}^{2} \frac{1}{\sqrt{t + \sigma_k^2}} \exp\left[-\frac{1}{2} \frac{(x_k - d_k)^2}{t + \sigma_k^2} \right] , \tag{A2}$$

$$\lambda \equiv -\frac{1}{2} \frac{N r_p}{\gamma} (1 + 1/\beta^2)$$

$$\approx -1.5 \times 10^{-11}\ \mathrm{m} \times \frac{N[10^{10}]}{E[\mathrm{TeV}]} \quad .$$

Components of the doublet, $\underline{\sigma}$ are the horizontal and vertical standard deviations of the bunch density, while $\underline{d}$ is its offset. These can, *and do*, depend on location, θ_{bb}. N is the number of particles in the bunch, and E is the (lab-frame) energy of a particle in it. The sign is chosen to correspond to p-$\bar{p}$ collisions; for p-p it would be positive.

Neglecting resonances, the first order expressions for the tunes are obtained by averaging $\partial H / \partial \underline{I}$ over all angles. The tune *shifts* are accordingly given by the following.

$$\Delta\underline{\nu} = \sum_{\theta_{bb}} \left\langle \frac{\partial U}{\partial \underline{I}} \delta_{2\pi}(\theta - \theta_{bb}) \right\rangle_{\theta,\underline{\phi}} = \sum_{\theta_{bb}} \frac{1}{2\pi} \left\langle \left. \frac{\partial U}{\partial \underline{I}} \right|_{\theta_{bb}} \right\rangle_{\underline{\phi}}$$

In the next sections we shall evaluate these averages, first for $\underline{d} = \underline{0}$ and then for the general case.

This is a bit formal, of course: not only does the Hamiltonian contain a delta function, but the integral expression is logarithmically divergent. (The potential energy of a line charge is infinite.) However, this does not present a problem, as only its derivatives are physically significant, and they are finite.

Tune shifts are obtained by differentiating with respect to the "action" coordinates, which means we must substitute for transverse coordinates from Eq.(A1) into Eq.(A2). When this is done, the exponential factors take the form,

$$\exp\left[-\frac{1}{2}\frac{x_k^2}{t+\sigma_k^2}\right] = \exp\left[-\frac{2\beta_k I_k \sin^2(\psi_k - \nu_k\theta + \phi_k)}{2(t+\sigma_k^2)}\right]$$
$$= \exp[\zeta_k(\cos 2\varphi_k - 1)] \quad ,$$

where $\zeta_k = \beta_k I_k / 2(t+\sigma_k^2)$ and $\varphi_k = \psi_k - \nu_k\theta + \phi_k$, and we have set $\underline{d} = \underline{0}$.

Following Bambade [1], we expand the exponent in a Fourier-Bessel series.

$$e^{\zeta(\cos 2\varphi - 1)} = Z_0(\zeta) + 2\sum_{n=1}^{\infty} Z_n(\zeta)\cos(n \cdot 2\varphi)$$

Here, $Z_n(\zeta) = e^{-\zeta} I_n(\zeta)$, where I_n is the modified Bessel function, $I_n(\zeta) = (-i)^n J_n(i\zeta)$. The integrand contains a product of two such series with differing arguments. Obviously, only the $n = 0$ term will survive angle-averaging, which gives us the result:

$$\Delta\underline{\nu} = \frac{\lambda}{2\pi} \sum_{\theta_{bb}} \int_0^{\infty} dt \frac{\partial}{\partial \underline{I}} \prod_{k=1}^{2} \frac{1}{\sqrt{t+\sigma_k^2}} Z_0(\zeta_k) \qquad \text{(A3)}$$

For purposes of numerical evaluation, it is best to change the integration variable to make the limits of integration finite. A choice which (a) takes the asymptotic behavior of the integrand into account and (b) is symmetric under interchange

of indices is $w \equiv 1/(1 + t/\sigma_1\sigma_2)$. With this it is convenient to introduce auxiliary functions, $\xi_1 \equiv 1 - w(1 - \sigma_1/\sigma_2)$, and similarly for ξ_2. It is easy to confirm that $w(t + \sigma_k^2) = \sigma_1\sigma_2\xi_k$ and $\zeta_k = (\beta_k I_k w/2\sigma_1\sigma_2\xi_k)$. The upshot is that Eq.(A3) is rewritten as follows.

$$\Delta\underline{\nu} = \frac{\lambda}{2\pi}\sum_{\theta_{bb}}\int_0^1 \frac{dw}{w\sqrt{\xi_1\xi_2}}\frac{\partial}{\partial\underline{I}}\left(Z_0(\zeta_1)Z_0(\zeta_2)\right)$$

In particular, evaluating the horizontal tune shift from a single beam-beam interaction gives us,

$$\begin{aligned}\Delta\nu_1 &= \frac{\lambda}{2\pi}\int_0^1 \frac{dw}{w\sqrt{\xi_1\xi_2}}\frac{\partial Z_0(\zeta_1)}{\partial I_1}Z_0(\zeta_2)\\ &= \frac{\lambda}{2\pi}\int_0^1 \frac{dw}{w\sqrt{\xi_1\xi_2}}\frac{\zeta_1}{I_1}[Z_1(\zeta_1) - Z_0(\zeta_1)]Z_0(\zeta_2)\\ &= \frac{\lambda}{4\pi}\frac{\beta_1}{\sigma_1\sigma_2}\int_0^1 \frac{dw}{\sqrt{\xi_1^3\xi_2}}Z_0(\zeta_2)\left[Z_1(\zeta_1) - Z_0(\zeta_1)\right]\end{aligned}$$

It is reassuring to check that the correct limit is achieved at small amplitudes. Setting $\underline{I} = \underline{0}$ we get,

$$\Delta\nu_1 = -\frac{\lambda}{4\pi}\frac{\beta_1}{\sigma_1\sigma_2}\int_0^1 dw/\sqrt{\xi_1^3\xi_2}\ .$$

Interestingly enough, this integral can be evaluated in closed form, which results in the usual small-amplitude beam-beam tune shift.

$$\begin{aligned}\Delta\nu_1 &= -\frac{\lambda}{2\pi}\frac{\beta_1}{\sigma_1(\sigma_1 + \sigma_2)}\\ &\approx \frac{1}{2\pi}\left(\frac{Nr_p}{\gamma}\right)\frac{\beta_1}{\sigma_1(\sigma_1 + \sigma_2)}\end{aligned}$$

FIGURES

FIG. 1. Separatrix of a $2\nu_1 - 2\nu_2$ resonance and island orbits.

FIG. 2. A projection of the separatrix for closed helix.

FIG. 3. Side view of representative orbits from stable regions (a) S_1 and (b) S_2.

FIG. 4. Appearance of the separatrix for low separator excitation.

FIG. 5. Appearance of the separatrix for higher separator excitation.

FIG. 6. Example of an almost phaselocked orbit near the separatrix of an irregular resonant orbit.

FIG. 7. Tori in the region associated with periodic orbits begin to "unravel" when the separation between beams is large.

FIG. 8. Histograms of encounter distances for orbits in the (a) "regular" and (b) "unravelling" regions.

REFERENCES

[1] P. Bambade. (a) *Effets faisceau-faisceau dans les anneaux de stockage e^+e^- a haute energie: Grossissement resonant des dimensions verticales dans le cas de faisceaux plats.* PhD thesis, Universite de Paris sud, Centre d'Orsay, 1984. LAL 84/21. (b) Improved analytical method for studying beam-beam driven nonlinear resonances. In Francis T. Cole and Rene Donaldson, editors, *Proceedings of the 12th International Conference on High Energy Accelerators. Fermilab*, August 11-16, 1983.

[2] Etienne Forest. A Hamiltonian-free description of single particle dynamics for hopelessly complex periodic systems. *Journal of Mathematical Physics*, 31:1133, 1990.

[3] ———- , Martin Berz, and John Irwin. Normal form methods for complicated periodic systems: A complete solution using differential algebra and Lie operators. *Particle Accelerators*, 24:91, 1989.

[4] Enrique Henestroza. Perturbative analysis of nonlinear betatron oscillations. Master's thesis, Massachusetts Institute of Technology, 1988.

[5] S. A. Kheifets and G. A. Voss. A kick experienced by a particle obliquely traversing a bunch. *Particle Accelerators*, 34:221–229, 1990.

[6] S. Krishnagopal and R. Siemann. Bunch-length effects in the beam-beam interaction. *Phys.Rev.D.*, page 2312, 1990.

[7] Leo Michelotti. Introduction to the nonlinear dynamics arising from magnetic multipoles. In Melvin Month and Margaret Dienes, editors, *Physics of Particle*

Accelerators. American Institute of Physics, 1987. AIP Conference Proceedings No. 153.

[8] ———-, Perturbation theory and the single sextupole. In Y. S. Kim and W. W. Zachary, editors, *The Physics of Phase Space.* Springer-Verlag, 1987.

[9] ———-, Resonance topology. In Eric R. Linstrom and Louise S. Taylor, editors, *Proceedings of the 1987 IEEE Particle Accelerator Conference.* IEEE, 1987.

[10] ———-, Beam-beam interaction effects. Technical Memo 1738, Fermilab, 1989. Viewgraphs presented at DoE review, August, 1989.

[11] ———-, Phase space concepts. In Melvin Month and Margaret Dienes, editors, *Physics of Particle Accelerators.* American Institute of Physics, 1989. A.I.P. Conference Proceedings No. 184.

[12] ———-, (a) MXYZPTLK: A C++ Hacker's Implementation of Automatic Differentiation. In G.Corliss and A.Griewank, editors, *Automatic Differentiation of Algorithms: Theory, Implementation, and Application.* SIAM, 1991. (b) MXYZPTLK: A practical, user-friendly C++ implementation of differential algebra: User's guide. Fermi Note FN-535, Fermilab, January 31, 1990.

[13] ———-, Exploratory orbit analysis. In Floyd Bennett and Joyce Kopta, editors, *Proceedings of the 1989 IEEE Particle Accelerator Conference.* IEEE, March 20-23, 1989. IEEE Catalog Number 89CH2669-0.

[14] ———-, and Selcuk Saritepe. (a) Exploratory orbit analysis of Tevatron helical upgrade: A first look. Technical report, Fermilab, 1989. Fermilab TM-1603. (b) Orbital dynamics in the Tevatron double helix. In Floyd Bennett and Joyce Kopta, editors, *Proceedings of the 1989 IEEE Particle Accelerator Conference,*

Chicago, IL. IEEE Press, March 20-23, 1989. Vol.2, pp.1391-1393.

[15] B. W. Montague. Fourth-order coupling resonance excited by space-charge forces in a synchrotron., October 1968. CERN ISR/68-38.

[16] R. D. Ruth, T. Raubenheimer, and R. L. Warnock. Superconvergent tracking and invariant surfaces in phase space. *IEEE Transactions on Nuclear Science*, NS-32(5):2206–2208, 1985.

[17] S. Saritepe, S. Peggs, and L. Michelotti. Long-range beam-beam interactions in the Tevatron: Comparing simulation to tune shift data. In *Proceedings of the 1990 European Particle Accelerator Conference, Nice, France.* pp.1667ff.

[18] Steven M. Stahl. *Beam Dynamics in the Fermilab Booster in the Presence of Space Charge.* PhD thesis, Northwestern University, June, 1991.

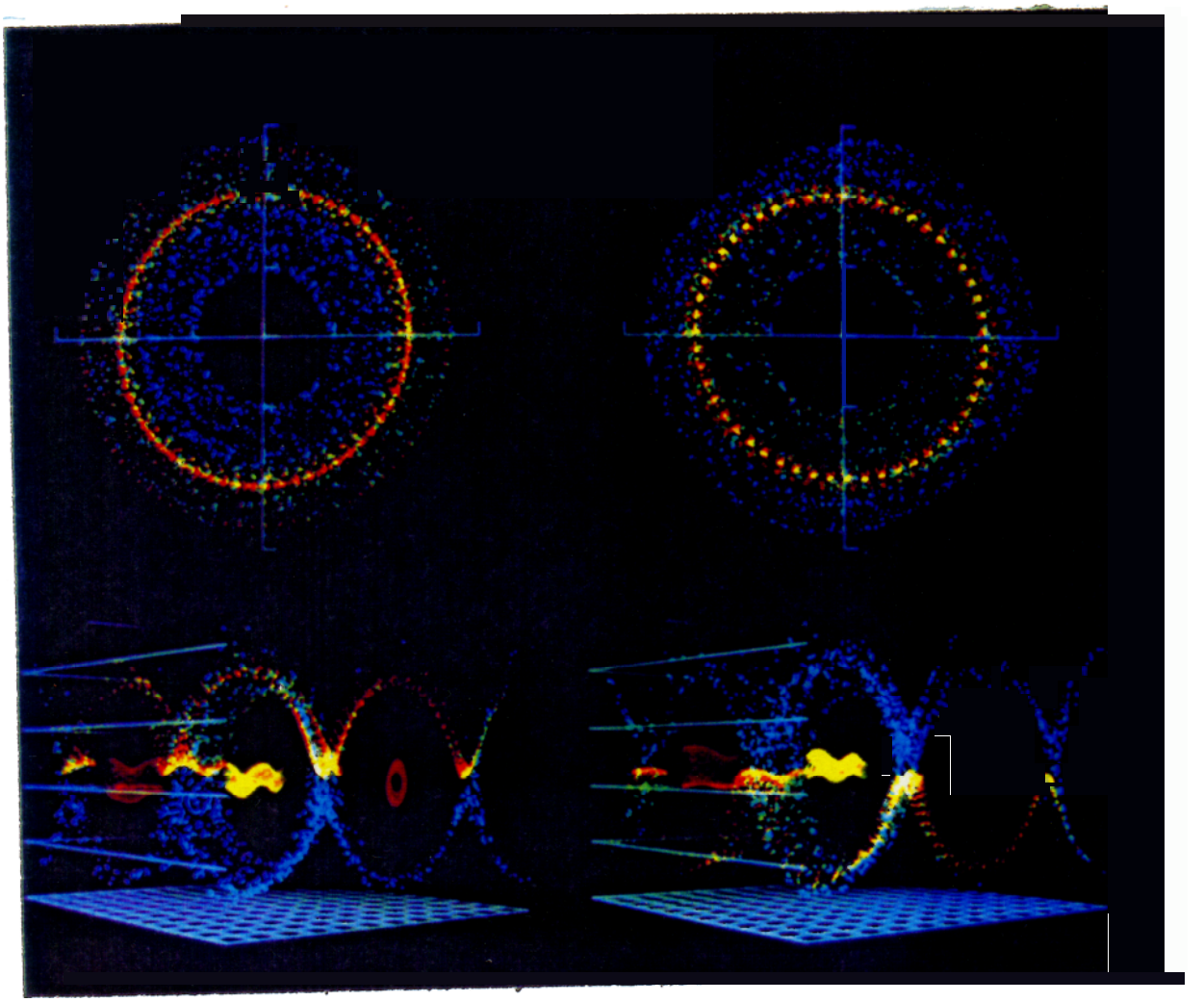

FIGURE 1

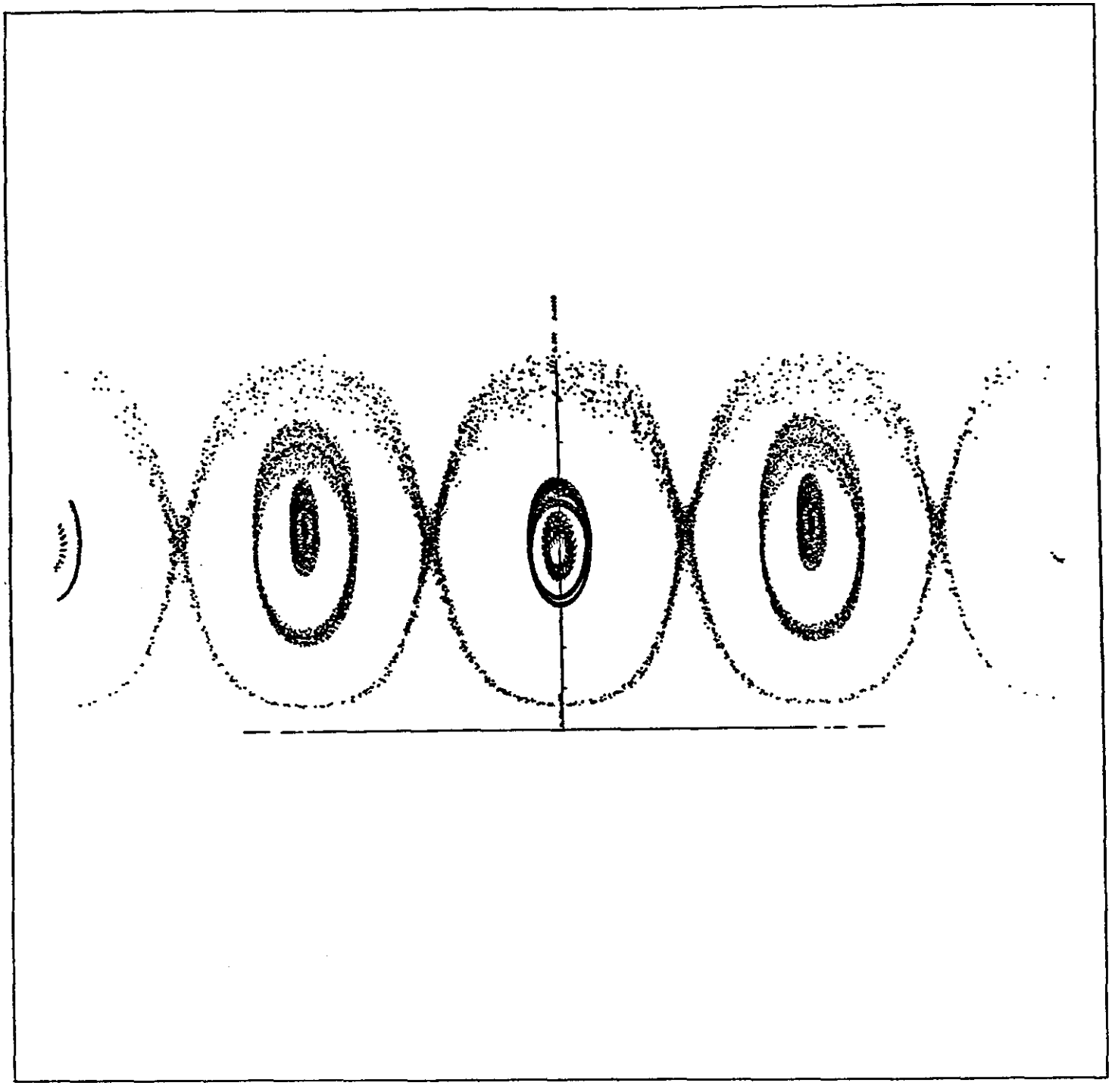

FIGURE 2

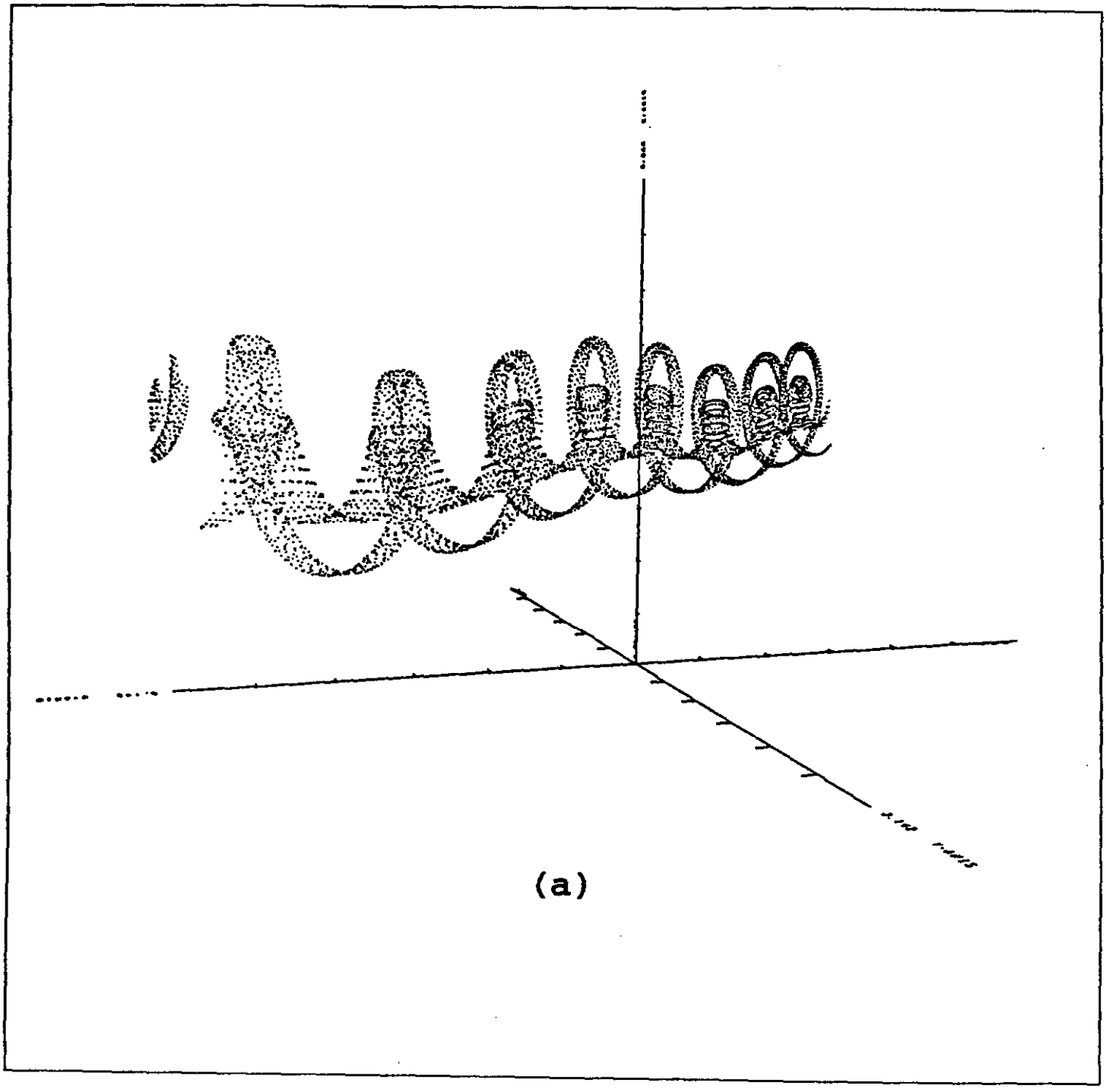

FIGURE 3(a)

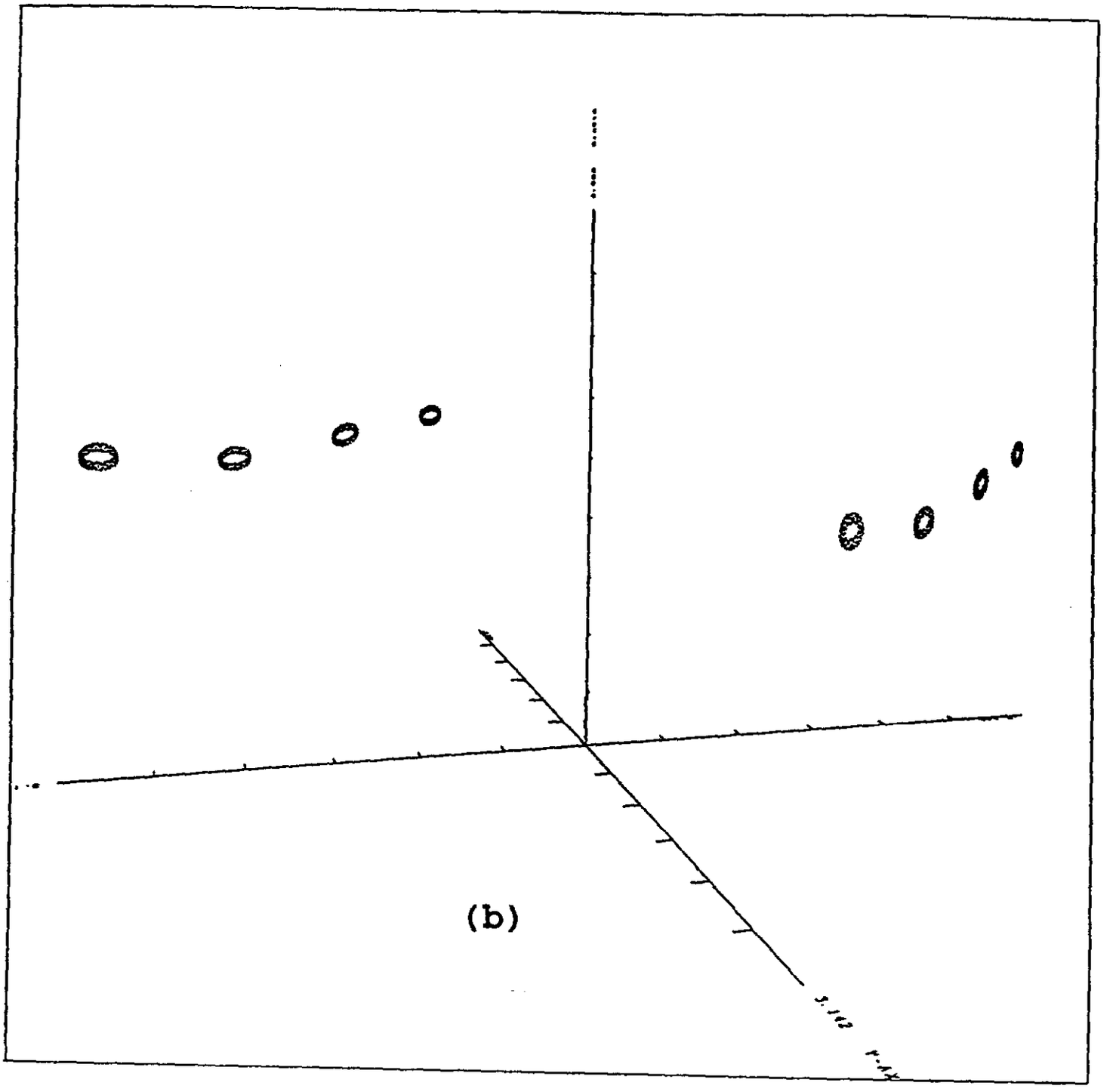

FIGURE 3(b)

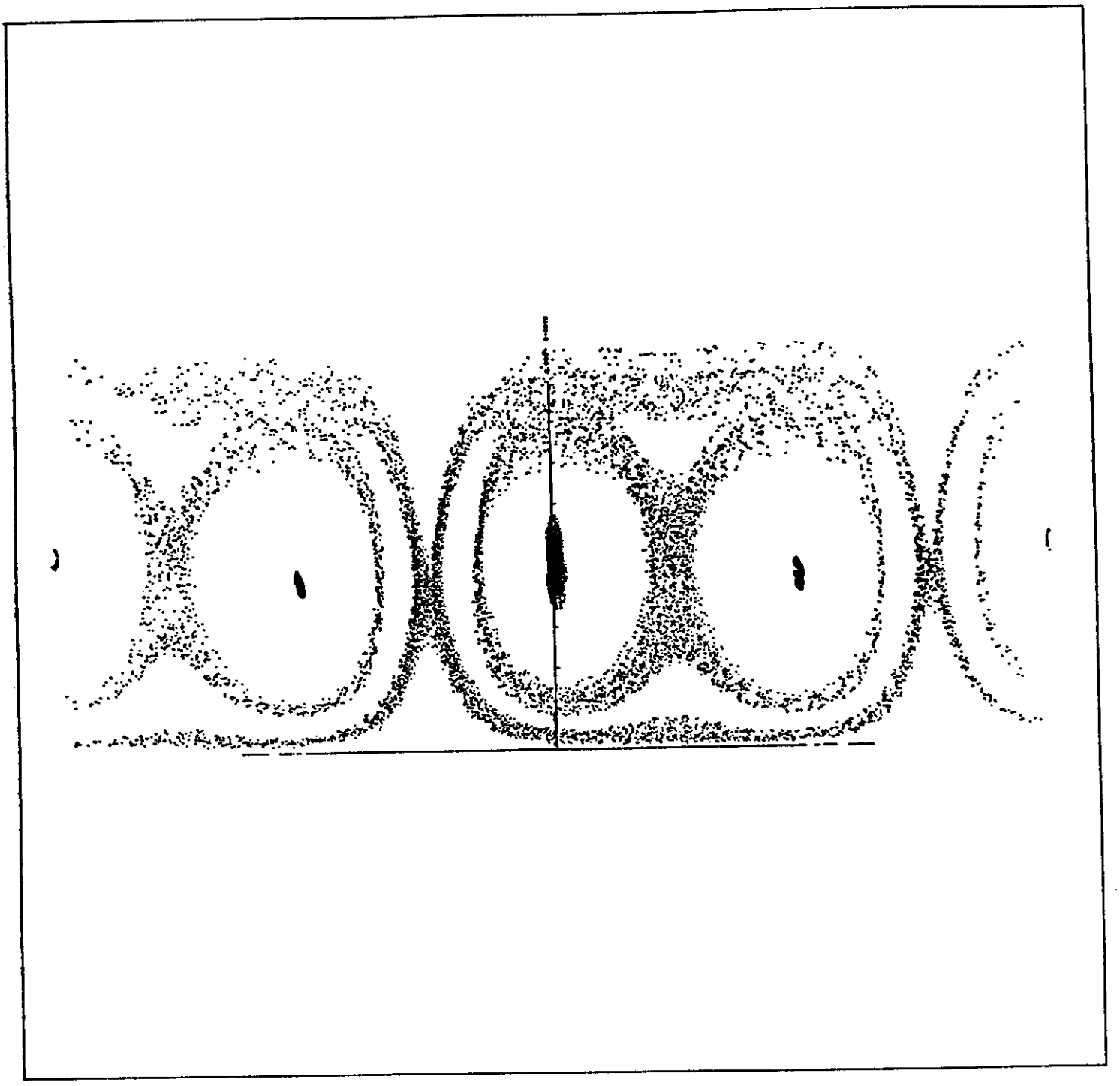

FIGURE 4

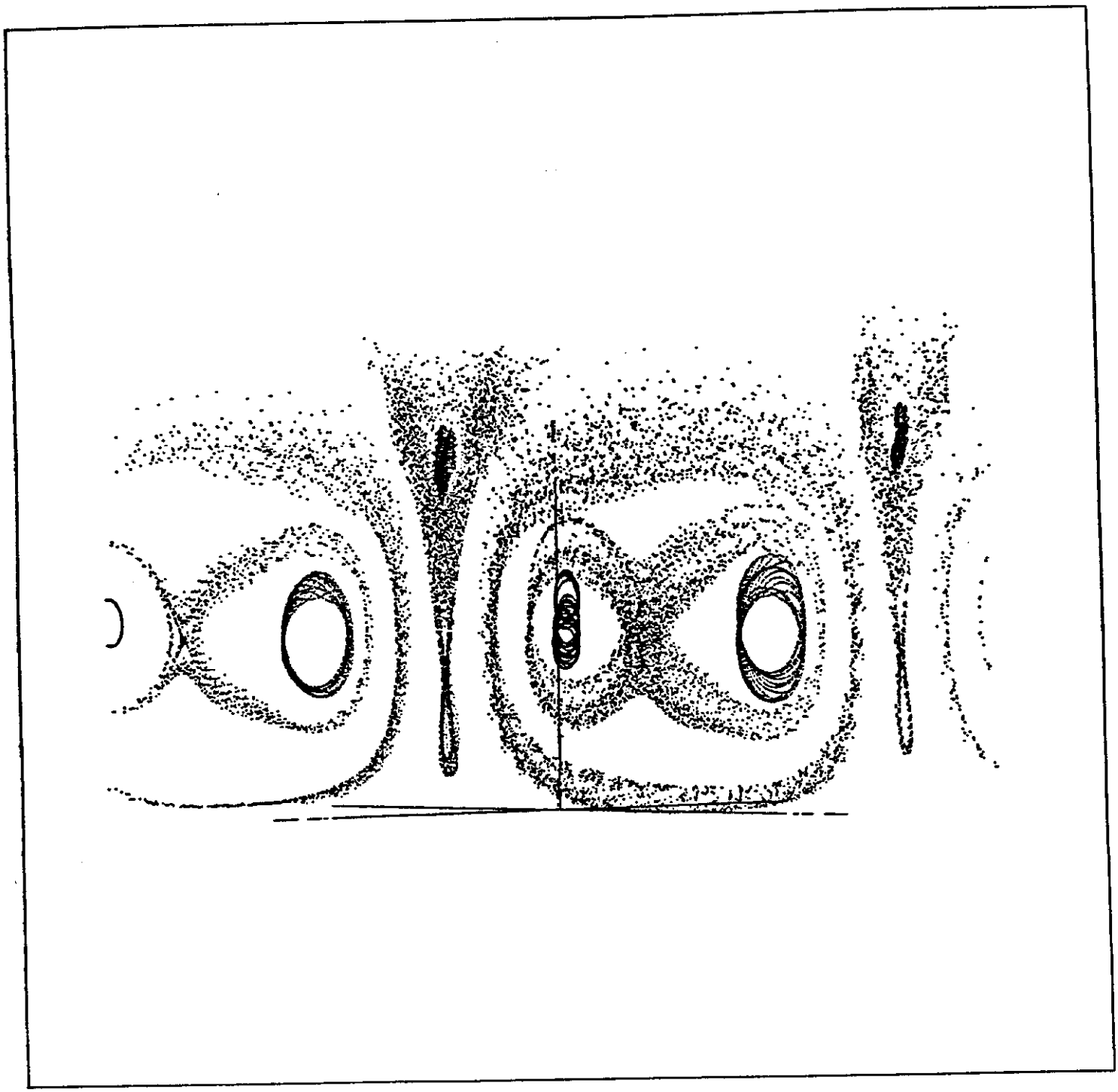

FIGURE 5

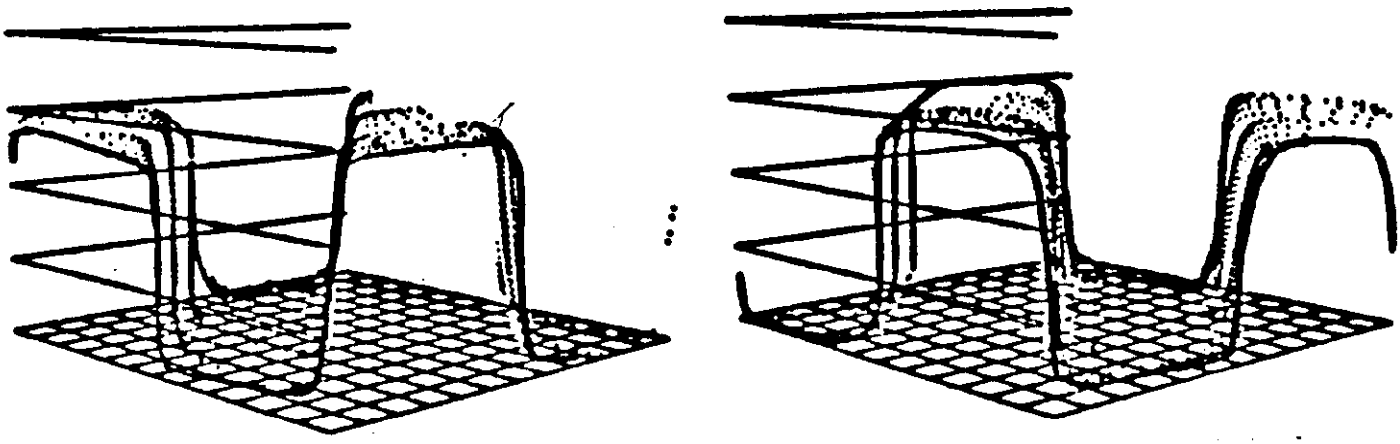

FIGURE 6

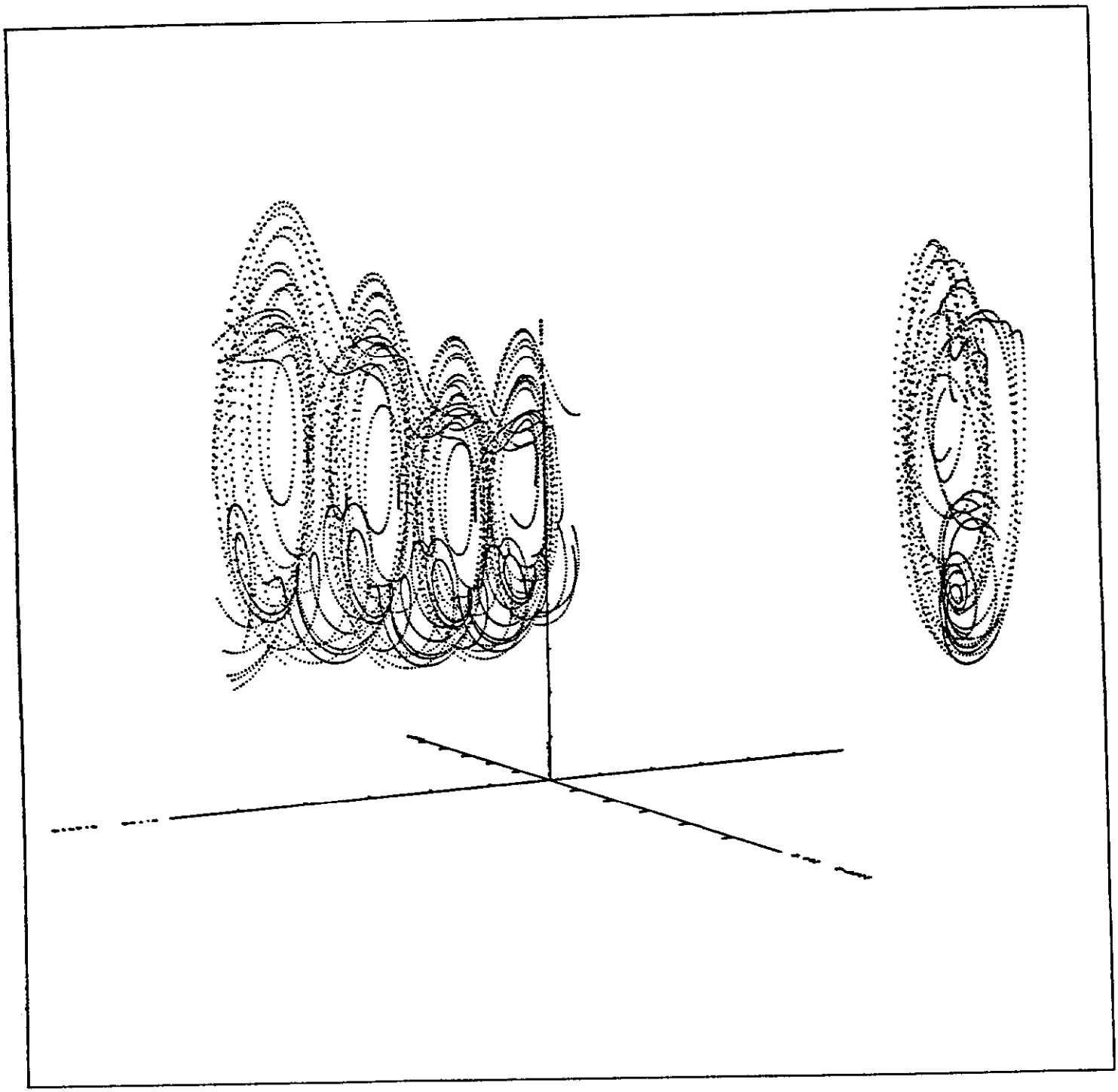

FIGURE 7

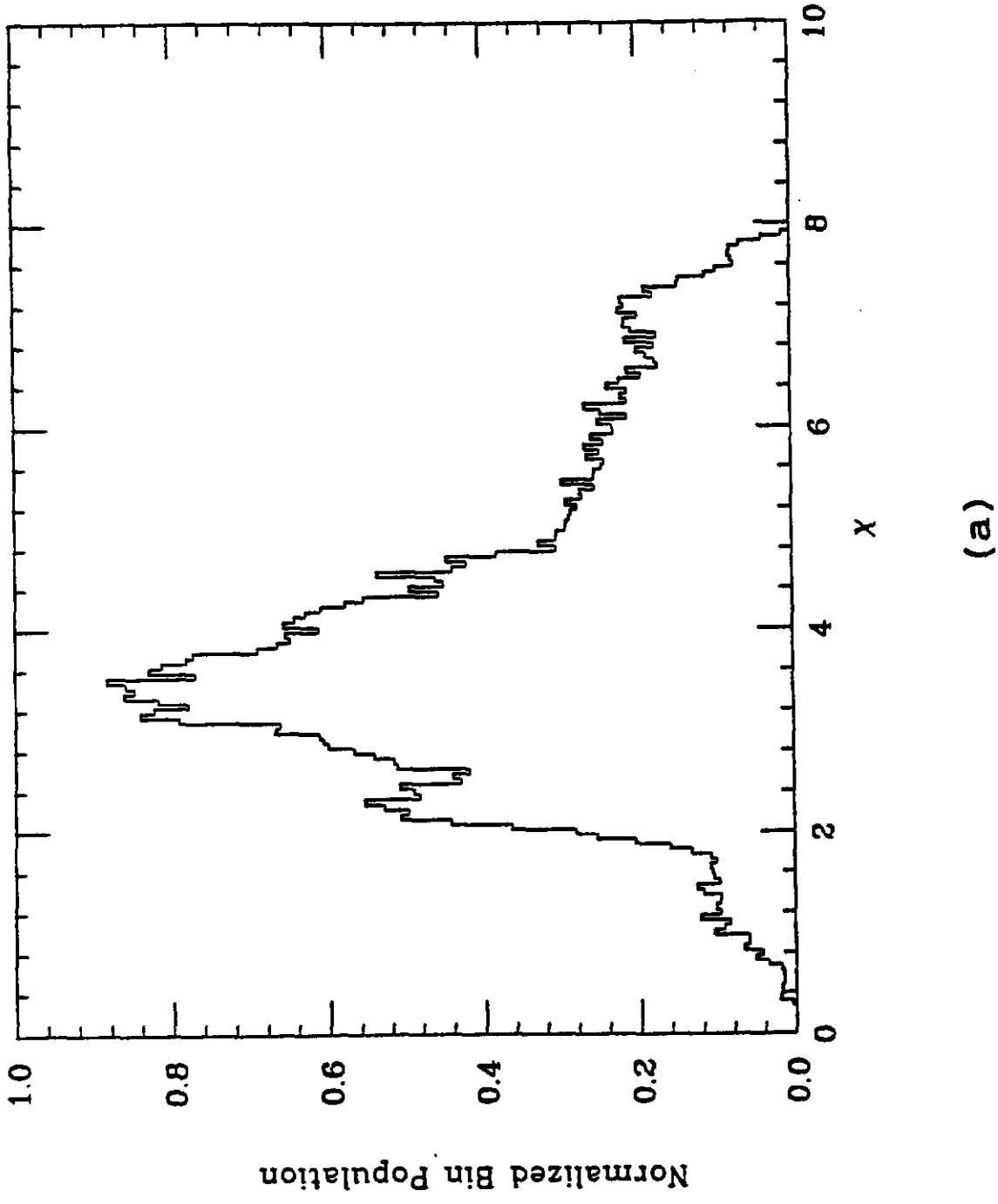

FIGURE 8(a)

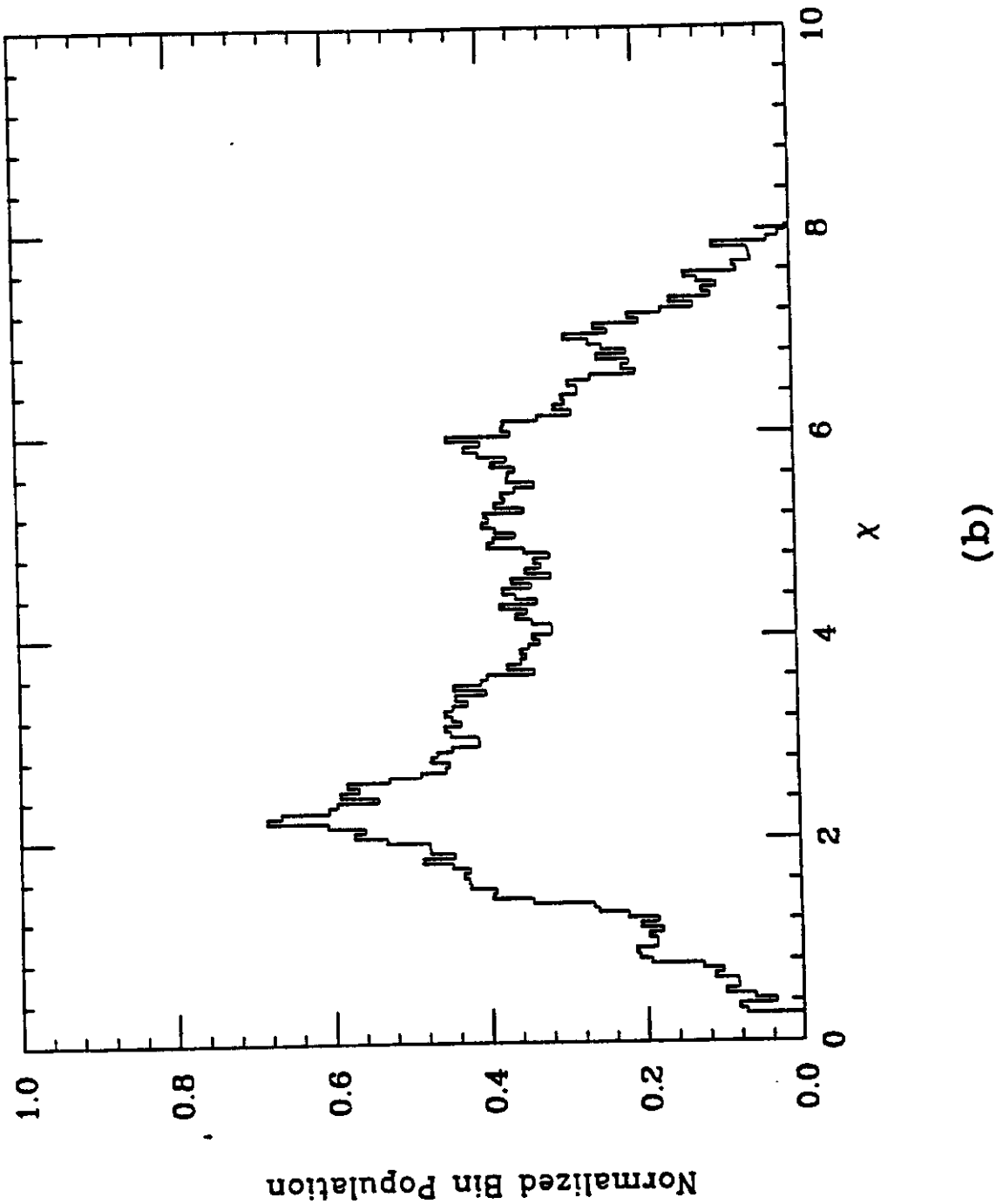

FIGURE 8(b)